Transactions of The Indian Institute of Metals
Vol. 62, Issues 4-5, August-October 2009, pp. 305-308

Phase-field simulation of micropores constrained by a solid network

A. Jacot, H. Meidani and M. Felberbaum

Computational Materials Laboratory, Ecole Polytechnique Fédérale de Lausanne, Station 12, Lausanne, Switzerland

Received 31 July 2009
Revised 12 October 2009
Accepted 13 October 2009
Online at www.springerlink.com

Keywords:
porosity; Aluminum; phase field modeling; pore pinching

Abstract

A 2D phase-field model has been developed in order to describe the morphology of a pore forming within interdendritic liquid channels and the geometrical effect of mechanical contacts with neighboring solid. The distribution of the solid, liquid and gas phases is calculated with a multiphase-field approach which accounts for the pressure difference between the liquid and gas phases, as well as diffusion of dissolved gases in the liquid. The model incorporates the perfect gas and Sievert's laws to describe the concentration and partitioning of gas molecules or atoms at the pore/liquid interface. The results show that the presence of solid can substantially influence the volume and pressure of the pore. A pore constrained to grow in narrow liquid channels exhibits a substantially higher mean curvature, a larger pressure and a smaller volume as compared with a pore grown under unconstrained conditions.

Introduction

Microporosity is one of the major defects encountered in solidification processes. The presence of micropores can considerably reduce the mechanical properties of a cast material, in particular the fatigue life and the ultimate tensile strength [1]. The basic mechanisms responsible for the formation of micropores are well established. Solidification shrinkage plays naturally a key role. If shrinkage cannot be compensated by liquid flow in the mushy zone due to limited permeability, large pressure drops will develop and lead to the formation of pores. Gas dissolved in the liquid metal, such as hydrogen in aluminum alloys, can substantially contribute or even govern the formation of micropores. Due to a lower solubility in the solid phase, gas concentrate in the remaining liquid as solidification proceeds and may reach the critical concentration for the nucleation of a bubble. Once a pore has nucleated, it becomes a sink for the gas supersaturated in the liquid phase and it will grow until thermodynamic equilibrium is reached.

Modeling the formation of porosity in castings has been a subject of research for several decades. The reader is invited to refer to the review article of Lee *et al.* [2]. State-of-the-art computer models describing the formation of microporosity on the scale of the casting process are based on volume-averaging methods for the calculation of the local temperature and pressure fields in the interdendritic liquid. These quantities are then used to estimate the level of gas segregation and to determine if conditions for the nucleation of a pore are met. After nucleation, the growth rate of the pores is calculated by solving a hydrogen mass balance.

One aspect that has not previously been examined is the effect of pore morphology, and more specifically, the radius of curvature which directly influences the gas pressure in the pore. As pores usually develop at high volume fractions of solid, they adopt complex shapes due to numerous contacts with neighboring dendrites arms. Only limited studies have been devoted so far to this effect, although it is potentially important. Direct observations by X-ray tomography have shown that the mean curvature can be larger than 0.2 μm^{-1}, which corresponds to a Laplace – Young overpressure of more than 400 kPa [3]. A preliminary phase-field approach for a numerical description of the morphology of a pore constrained by a dendritic network was also presented in [3]. One of the limitations of this study was the fact that the influence of the solid was taken into account through the geometry of the calculation domain, which contained only liquid and gas phases, but was considered to be surrounded by solid. With such a method, only simple solid shapes could be described since the solid/liquid or solid/gas interfaces had to correspond to the boundaries of the orthogonal calculation grid. The present work is an extension of the approach presented in [3] based on a multiphase-field formulation. The method allows for a description of micropores constrained in a solid network having a more realistic shape.

Model

A multiphase field model has been developed in order to describe the shape of a pore forming within an interdendritic liquid channel and the geometrical effect of mechanical contacts with neighboring solid. The problem is solved in a domain that is representative of a small section of a dendritic network. The presence of solid, liquid and pores is described through the phase-field variables ϕ_s, ϕ_l, ϕ_p, which can be understood as local volume fractions. These variables are linked together by the condition $\phi_s+\phi_l+\phi_p = 1$.

The evolution of the phase-field variables is calculated by solving the following equations:

$$\dot{\phi}_i = \sum_{k \neq i} M_{ik} \begin{bmatrix} \varepsilon_{ik}^2 \left(\phi_k \nabla^2 \phi_i - \phi_i \nabla^2 \phi_k \right) \\ -2W_{ik} \phi_k^2 (1-\phi_k)^2 \phi_i (1-\phi_i)(1-2\phi_i) \\ -30 \phi_i \phi_k (1-\phi_i)(1-\phi_k) \Delta G_{ik} \end{bmatrix} \qquad (1)$$

$$k, i = l, s, p$$

with

$$\Delta G_{sl} = \Delta s_f \Delta T \qquad (2a)$$

$$\Delta G_{lp} = p_p - p_l \qquad (2b)$$

$$\Delta G_{sp} = 0 \qquad (2c)$$

and

$$W_{ik} = \frac{15\sqrt{2\gamma_{ik}}}{\delta_{ik}} \qquad (3a)$$

$$\varepsilon_{ik}^2 = 2W_{ik}\delta_{ik}^2 \qquad (3b)$$

$$M_{ik} = \frac{\mu_{ik}}{\delta_{ik}} \qquad (3c)$$

where p_p is the pressure in the pore, p_l is the pressure in the liquid, Δs_f is the entropy of melting, and ΔT is the undercooling. The parameters μ_{ik}, W_{ik}, δ_{ik}, and γ_{ik} correspond respectively to the interface mobility coefficient, the double-well height, the interface thickness and the interfacial energy of the interface between phases i and k.

These equations are similar to the multiphase-field model of solidification of [4]. A noteworthy difference is the form of the polynomial expressions used for the double well and driving force terms, which have been modified to avoid the systematic presence of the third phase in the interfaces. For $\phi_i = 0$ and $\nabla\phi_i = 0$, Equation 1 yields $\dot{\phi}_i = 0$, whatever ϕ_j and ϕ_k (j and $k \neq i$), which is the mathematical condition to be satisfied for phase i not appearing spontaneously in a j/k interface.

Another aspect to be mentioned is the driving force for the liquid/pore transformation, which is given by the pressure difference between the interior of the pore and the surrounding liquid (Eq. 2b). This expression can be justified by solving the steady-state form of Eq. 1 in cylindrical coordinates for a system composed of a single pore surrounded by liquid. By doing so, one can show that the Laplace pressure condition, $p_p - p_l = 2\gamma_{lp} / r_p$, where r_p is the pore radius, is recovered.

In this preliminary approach, the growth kinetics are assumed to be governed by hydrogen diffusion in the liquid, which, as pointed out by Lee and Carlson [5,6], can be the limiting factor. (Hereafter the gas responsible for porosity will always be referred to as hydrogen, although the model could apply to other systems as well). A local volumetric molar concentration of hydrogen is introduced based on an averaging procedure and considering the phase-field variables as local volume fractions:

$$c^H = \phi_s c_s^H + \phi_l c_l^H + \phi_p c_p^H \qquad (4)$$

where c_s^H, c_l^H and c_p^H are volumetric molar concentrations of hydrogen in the solid, liquid and gas, respectively.

Assuming thermodynamic equilibrium at the interface, c_s^H and c_l^H can be expressed as a function of p_p using Sievert's law:

$$c_s^H = S_s \sqrt{\frac{p_p}{p_0}} \qquad (5a)$$

$$c_l^H = S_l \sqrt{\frac{p_p}{p_0}} \qquad (5b)$$

where S_s and S_l are the Sievert's constants (in atomic moles/m^3) for the solid and liquid, respectively, and p_0 is the standard pressure. Introducing also the perfect gas law, Eq. 4 can be rewritten as:

$$c^H = \left(\phi_l S_l + \phi_s S_s \right) \sqrt{\frac{p_p}{p_0}} + \phi_p \frac{2p_p}{RT} \qquad (6)$$

A hydrogen conservation equation is then solved, neglecting any hydrogen concentration gradient in the gas phase and any hydrogen transport in the liquid due to flow:

$$\frac{\partial c^H}{\partial t} = \nabla \cdot \left(\phi_s D_s^H \nabla c_s^H + \phi_l D_l^H \nabla c_l^H \right) \qquad (7)$$

The resolution of Eqs 1 and 7 is performed using a finite difference method and an explicit time-discretization scheme. At each time-step, the solution of Eq. 7 is used to calculate the driving force terms of the phase equations. This requires solving the second order polynomial expression of Eq. 6 to obtain p_p from c^H. An averaging procedure eliminating any concentration gradient in the pore is applied at every time-step. To ensure numerical stability, the time-step is determined so as to satisfy the Fourier condition of both Eqs 1 and 7, using a Fourier number of 0.1 rather than 1/4: $D_s \Delta t / h^2 < 0.1$, $M_{ik} \varepsilon_{ik}^2 \Delta t / h^2 < 0.1$, where h is the mesh size.

Results and Discussion

A first test was carried out in order to verify the capability of the model to correctly calculate the pressure and the radius of a spherical pore for a given set of conditions in terms of hydrogen content in the calculation domain, c_0, hydrogen solubility, S_l, and liquid pressure, p_l. The calculation was performed in a 2D square domain containing only liquid except for a small pore of arbitrary radius located at the center. No solid was considered in this first test. Once steady state was reached, the pore radius, r_p, and the pore pressure, p_p, were compared with the analytical solution obtained by solving the following set of equations:

$$c_l^H = S_l \sqrt{\frac{p_p}{p_0}} \qquad (8a)$$

$$p_p = \frac{c_p^H}{2} RT \qquad (8b)$$

$$p_p - p_l = \frac{\gamma_{lp}}{r_{eq}} \qquad (8c)$$

$$\pi r_{eq}^2 c_p^H + \left(V_{comp} - \pi r_{eq}^2 \right) c_l^H = V_{comp} c_0 \qquad (8d)$$

where r_{eq} is the equilibrium radius of the circular pore and V_{comp} is the volume of the calculation domain.

Table 1 summarizes the different parameters used in the calculation. The calculation was started with an initial pore size about 10 times smaller than r_{eq}. In the initial state, the liquid is supersaturated in hydrogen. The pore is thus expected to grow.

Table 1: parameters used in the phase-field calculations.

Parameter, unit	*Numerical Value*
Mesh size [m]	2.5×10^{-8}
δ [m]	2.0×10^{-7}
V_{comp} (without solid) [m^2]	1.5×10^{-10}
p_0 [Pa]	101325
p_1 [Pa]]	101325
T [K]	1000
M_{ls} [m^2s/kg]	1×10^{-6}
D_1 [m^2/s]	1×10^{-6}
S_l [mol/m^3]	0.69
γ_{lp} [J/m^2]	0.8
γ_{sp} [J/m^2]	0.8
γ_{ls} [J/m^2]	0.4
c_0[mol m^{-3}]	20.0
Typical CPU time	20 h

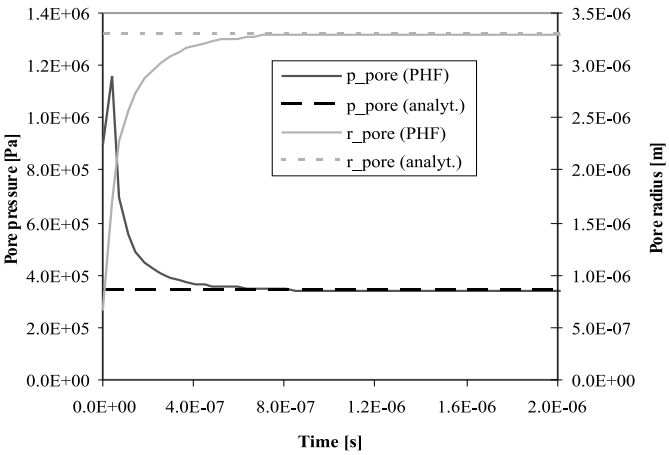

Fig. 1 : Radius and pressure of a circular 2D pore calculated with the phase-field model (PHF) and with the analytical solution for a hydrogen solubility in the liquid of S_l = 0.69 mol/m^3 and an overall hydrogen content, c_0, of 20 mol/m^3.

As can be seen in Fig. 1, the pore radius calculated with the phase-field model increases rapidly, whereas its pressure globally decreases, until a steady-state is reached at a time of about 1×10^{-6} s. Both the pressure and the radius of the pore stabilize very close to the analytical solution. Similar calculations started with different pore radii, either larger or smaller than r_{eq}, yielded the same steady state solution. Thus, the phase-field model is capable of correctly describing a bubble in equilibrium with its surrounding liquid, satisfying simultaneously the mechanical and chemical equilibrium conditions.

The transient regime of the calculation corresponds to the time required to homogenize the hydrogen concentration in the liquid. Although hydrogen diffusion can be the limiting factor for pore growth, the transient regime of the simulation cannot be exploited quantitatively in this preliminary approach. The reason is that the liquid flow induced by the expansion of the bubble, and thereby hydrogen transport by convection, are not considered in the simulation. For this reason only the steady state solutions of the simulation will be analyzed hereafter.

The model was then used to investigate the morphology and the pressure in a pore growing under the constraint of a surrounding solid. The calculations were performed in 2D domains containing a series of liquids channel separated by dendrites arms (see Fig. 2). Each solid structure is characterized by a different dendrite arm spacing, λ = 2.5, 3.75 or 5 μm. The widths of the liquid channels where the pore can grow are proportional to λ. In this preliminary work, only the evolution of the liquid/gas interface was considered and the hydrogen solubility in the solid was ignored. The parameters M_{ls}, M_{sp}, D_s^H and S_s were therefore set to zero. As the solid is considered as inert, the calculation were carried out using identical volumes of liquid, and a nominal concentration of c_0 = 20 atomic mol/m^3 in the liquid prior to pore nucleation.

The calculations were initialized with a relatively small pore located at the center of the calculation domain and without any contact with the solid. Since the liquid is supersaturated in hydrogen, the pore grows until equilibrium is reached. The initial shape, some transient state and the final shapes of the pore are shown in Fig. 2 for the three different arm spacings, λ. As can be seen the pore develops in a non-symmetric way, and may move to a more open space in order to reduce its curvature and thereby its internal pressure.

The pressure, the mean radius of curvature (which is averaged over the liquid/pore interfaces only) and the equivalent radius of the pore (which is defined as $\sqrt{A_p/\pi}$

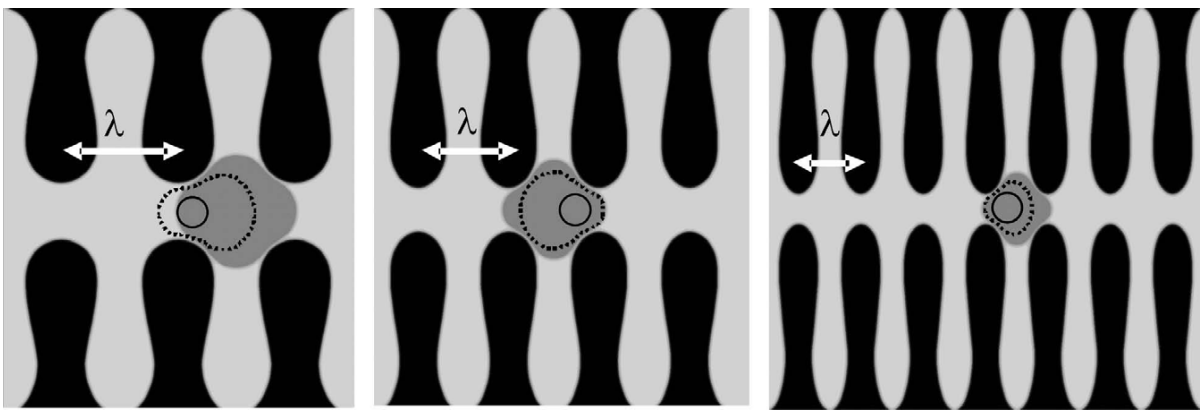

Fig. 2 : Initial (black circle), transient (dotted line) and equilibrium (grey/orange fill) pore shapes for different arm spacings, l = 5, 3.75 and 2.5 μm.

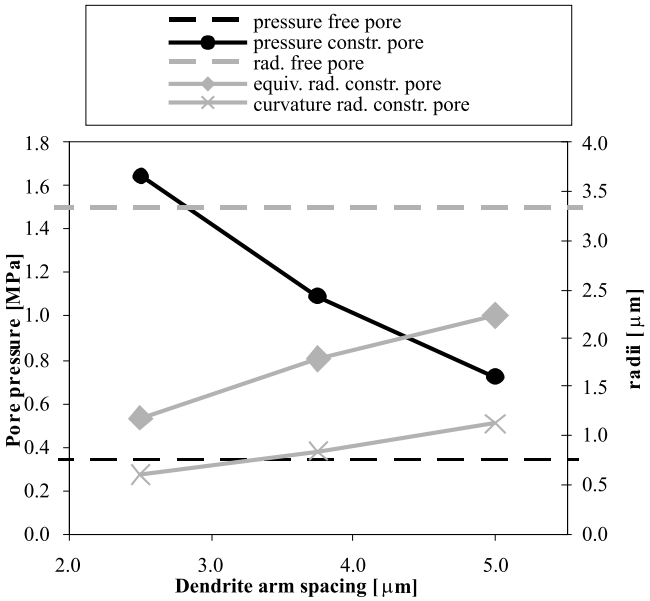

Fig. 3 : Effect of dendrite arm spacing on pore pressure and pore radii calculated with the phase-field model. The dashed lines represent the pressure and the volume of an unconstrained pore for the same conditions.

where A_p is the area of the pore) were extracted from the calculations for the final state and are presented in Fig. 3. As can be seen, a smaller dendrite arm spacing leads to a higher pressure, a smaller radius of curvature and a lower pore volume (i.e. smaller equivalent radius), as compared with a less constrained pore. This effect is directly related to the fact that the growth of a pore inside a narrow liquid channel requires highly curved gas/liquid interfaces in order to satisfy the mechanical equilibrium at the *s/l/p* triple junctions, which is defined by the interfacial energies γ_{ls}, γ_{sp}, and γ_{lp}. The pressure is consequently larger in such pores since the Laplace - Young equation has to be satisfied.

In the calculations shown here the influences of the solid morphology on the volume fraction and the morphology of the pores is substantial. By dividing the liquid channel width by a factor 2, the pressure raises and the equivalent radius drops by a similar factor. The magnitude of this effect is naturally linked to the fact that the channel widths used in the calculations are rather small. However such narrow liquid channels are not unrealistic at the end of solidification.

Conclusion

A 2D phase field model has been developed in order to describe the morphology of a pore forming within interdendritic liquid channels and the geometrical effect of mechanical contacts with neighboring solid. The results show that the presence of solid can substantially influence the volume and pressure of the pore. A pore constrained to grow in narrow liquid channels exhibits a larger pressure, and a smaller volume as compared with a pore grown under unconstrained conditions due to a higher mean curvature.

Although the model accounts for hydrogen diffusion in the liquid, which is one of the main aspects governing the growth kinetics of a pore, this approach does not allow at this stage to correctly describe the dynamics of pore formation. To do so, the model should be combined with a description of the liquid flow induced by the pore growth. This would permit to properly take into account the effect of hydrogen transport by convection. In order to make a more quantitative investigation of the influence of the solid on the pore morphology the approach should be extended to 3D and the evolution of the solid/liquid interface should be considered.

References

1. Campbell J, *Castings*, Butterworth-Heinemann Ltd; 2nd Ed., 2003.
2. Lee P D, Chirazi A and See D, *Journal of Light Metals*, **1**(1) (2001) 15.
3. Felberbaum M and Jacot A, *Modeling of Casting, Welding, and Advanced Solidification Processes - XII*, ed. by Cockcroft S L and Maijer D M, TMS, (2009) 369.
4. Tiaden J, Nestler B, Diepers H J and Steinbach I, *Physica D*, **115** (1998), 73-86.
5. Lee P D and Hunt J D, *Acta Materialia*, **45**(10) (1997) 4155.
6. Carlson K D, Lin Z and Beckermann C, *Metall. Mater. Trans. B*, **38**(4) (2007) 541.